2022 NDIA MICHIGAN CHAPTER
GROUND VEHICLE SYSTEMS ENGINEERING
AND TECHNOLOGY SYMPOSIUM
AUTONOMY, ARTIFICIAL INTELLIGENCE ROBOTICS (AAIR) TECHNICAL SESSION
AUGUST 16-18, 2022 - NOVI, MICHIGAN

RPV DETERMINATION FOR HEAVY TRUCK PLATOONING APPLICATIONS USING IR AND RGB MONOCULAR CAMERA

Tyler Flegel[1], **Howard Chen, PhD**[1], **David Bevly, PhD**[1]

[1]Department of Mechanical Engineering, Auburn University, Auburn, AL

ABSTRACT

Many significant advances have been made in autonomous vehicle technology over the recent decades. This includes platooning of heavy trucks. As such, many institutions have created their own version of the basic platooning platform. This includes the California PATH program [1], Japan's "Energy ITS" project [2], and Auburn University'sCACC Platform [3]. One thing these platforms have in common is a strong dependence on GPS based localization solutions. Issues arise when the platoon navigates into challenging environments, including rural areas with foliage which might block receptions, or more populated areas which might present urban canyon effects. Recent research focus has shifted to handling these situations through the use of alternative sensors, including cameras. The perception method proposed in this paper utilizes the You Only Look Once (YOLO) real-time object detection algorithm in order to bound the lead vehicle using both RGB and IR cameras. Range and bearing are determined using various methods. The methods are then tested on real world data.

Citation: T. Flegel, H. Chen, D. Bevly, "RPV Determination for Heavy Truck Platooning Applications Using IR and RGB Monocular Camera," In *Proceedings of the Ground Vehicle Systems Engineering and Technology Symposium* (GVSETS), NDIA, Novi, MI, Aug. 16-18, 2022.

1. INTRODUCTION

Platooning can be defined as a convoy of 2 or more vehicles, in which the first is manually driven by an operator. There are many advantages to such a setup. This includes a reduction in the number of drivers required to operate the platoon while also increasing the fuel efficiency of all vehicles in the platoon, including the lead vehicle [4]. Platooning platforms often have a strong dependence on GPS based solutions such as Dynamic Real Time Kinematic (DRTK) to provide localization with centimeter level accuracy [5]. Due to this dependence, issues arise when platoons enter areas that do not have clear GPS signals. Platoons also face issues with multipath errors, which occur when GPS signals are reflected off of surfaces and cause invalid GPS solutions. Real Time Kinematic (RTK) based solutions are especially vulnerable

to multipath errors [6]. Additionally, RTK-based solutions fail when even one truck in the platoon loses GPS reception. These limitations with GPS have shifted research focus to solutions which do not rely on a GPS solution for platoons to function properly. Sensors including Lidar, Radar as well as monocular and stereoscopic cameras can be used as alternatives to GPS. *Lidar* is effective at generating point clouds which can be used for identifying and determining range to a lead vehicle; however, Lidar is more expensive than the other options. Radar is commonly used for Adaptive Cruise Control in both commercial and privately owned vehicles. However, the methods employed simply detect range to the vehicle ahead, and do not contextualize the points. This would be required for sophisticated path following, such as for a lane change. Traditionally, for vision problems requiring range, stereo cameras are the sensor of choice. However, stereo cameras have some drawbacks. In general, they are more expensive than monocular cameras. Additionally, stereo cameras require the use of an algorithm, which solves the correspondence problem, to generate depth maps. When tracking objects that are far away, relative to the distance between the two cameras, the method can fail [7]. The algorithm can also fail when dealing with objects and environments that don't have enough detectable features. Monocular cameras are inexpensive, and readily available. RGB cameras are the most popular Monocular camera, and capture visible light. IR monocular cameras record infrared light instead of visible light. This makes it possible for them to function at night. They are also more resilient to dust and weather effects than their RGB counterparts.The purpose of this paper is to evaluate methods for estimating the Relative Position Vector (RPV) to a leader vehicle in platoon through the use of a monocular camera (IR and RGB) on real world data.

2. BACKGROUND

2.1. Platooning Overview

The basic control structure followed by most platooning platforms can be seen in *figure 1*. The lateral controller manipulates the steering angle of the follower vehicle. The longitudinal controller controls the acceleration of the following vehicle to track a desired following distance from the lead vehicle. Auburn University's longitudinal controller accepts range and range rate as inputs. These measurements are estimated by a range estimator which uses a RPV provided by DRTK, and range and range rate from Radar. The lateral controller utilizes a "bread-crumb" following approach which considers range and bearing angle in time to place GPS waypoints.

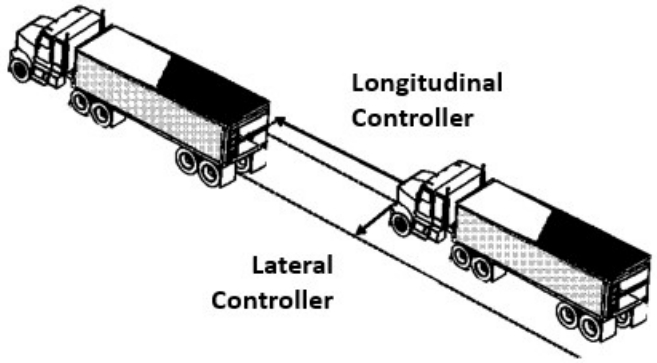

Figure 1: **Controllers Used in Traditional Platooning Platform** - Lateral Controller: controls steering angle and accepts an estimated path taken by lead vehicle as input. Longitudinal Controller: controls acceleration and accepts input as range and range rate, provided by GPS, Radar, Lidar, and stereoscopic and monocular cameras

2.2. Object Detection and Tracking

In computer vision, object detection and tracking is considered to be a class of problem focused on recognizing and annotating instances of objects over consecutive image frames. There are two primary options for convolutional neural networks (CNN)

which perform object detection and tracking: You Only Look Once (YOLO) [8] and the Region-Based CNN (RCNN) [9]. Using YOLO has many advantages, including how fast the algorithm can run. Additionally, because YOLO analyzes the input image in its entirety, the algorithm can leverage contextual information in its class prediction [8]. These advantages have made YOLO one of the most popular options for object and tracking applications. The working principles of the YOLO algorithm can be seen in *figure 2*. Each bounding box is accompanied by 5 states: width of bounding box, height of bounding box, x-coordinate in the image frame, y-coordinate in the image frame, and class label. Some updates have been provided to YOLO in 2018 with the release of YOLOv3 [10], which is used in this paper. Tiny Yolo is also utilized, which has a smaller network architecture allowing the algorithm to run faster. The tradeoff between accuracy and algorithm speed is considered later in this paper.

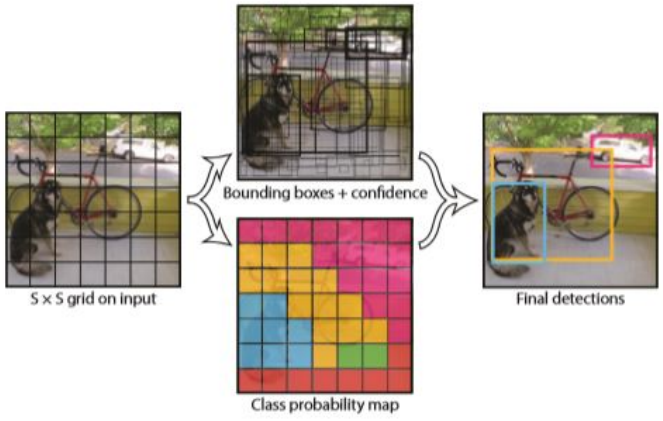

Figure 2: **YOLO Algorithm [8]** - Division of image into *SxS* grid, Hypothesis bounding boxes generated while simultaneous grid probability determined for each cell, Using the hypothesis bounding boxes and probabilities output final detections are generated.

3. RELATED WORK

3.1. Scale Platooning Platforms

Due to the costs and logistics associated with having and maintaining a full scale platooning platform, much of the research on platooning has been done with scale platooning platforms. This extends to platooning with monocular camera. Rezgui et al. [11] developed a platform that used Tiny YOLO to bound the lead vehicle, and determine range from ultrasonic sensors. The robot's wheel speed commands were determined based on the lead vehicle's x-coordinate in the image frame [11]. A similar scale platooning platform was developed in [12], that instead used a DNN to bound the lead vehicle. The size of the bounding box was used to control the speed of the follower vehicle. The steering angle was determined in a similar fashion to [11]. Another example is [13] which used a classical HSV (Hue Saturation Value) filter to bound the lead vehicle. The range was determined using a derived function from the area of this bounding box. The inter—vehicular angle was determined using the lateral offset and range. Theinert et al.[14] used a similar method, except mounted an illuminated sphere to the rear of the lead vehicle which was detected using classical methods. Additionally, the pinhole camera model was used to get range . Mitchell et al. [15] detected a mock license plate using a Pixy Camera to get range. Another clever use for the YOLO framework was in [16], which not only detected the lead vehicle, but used an LED light matrix to communicate specific vehicle states to the follower.

3.2. Full-Scale Platooning Platforms

While most of the work on monocular based platooning has been on scale platforms, it has been extended to full-scale platforms. Kim et al. [17] used YOLO to detect the lead vehicle, as well as other vehicles on the road way. In the methodology, RADAR was used to get range, and this range was used to generate a platooning specific lane following

algorithm. [18] used YOLOv3 in tandem with a dedicated keypoint localization network to estimate lead vehicle states.

Some work has been done on Infrared Platooning. Woeber et al.[19] evaluated the accuracy of the AdaBoost detection algorithm on thermal imagery of heavy trucks, but did not determine range or bearing to the vehicle.

Another popular approach to the monocular platooning problem involves using a predefined 3D model or template of the lead vehicle, defining features on the model, and then finding these features in real time to determine pose using classical computer vision [20][21][22][23].

3.3. Other YOLO Ranging Applications

Outside platooning applications, YOLO has been used to get monocular range. A collision warning system which used YOLO outputs as the input to a secondary neural network to determined range to pedestrians and street vehicles for locomotives. A secondary neural network was trained to determine the range to the detected entities [24]. YOLO has also been utilized to detect street signs [25]. The range to the signs were determined using the size of the bounding box.

3.4. Monocular Ranging

Monocular cameras have been utilized for Adaptive Cruise Control , getting range and range rate [26]. As well as for a forward collision warning system [27]. The method doesn't utilize the pinhole camera model, instead estimating a virtual horizon line. This work was extended in [28], which leveraged lane detection to estimage parameters.

3.5. Contributions

This work serves to evaluate monocular platooning on a full-sized platooning platform, through various road conditions. To get range, the classical pinhole model is evaluated as well as the virtual horizon model from [27]. Bearing is also determined through methods previously only evaluated on scale platooning models to the best of our knowledge. Additionally, the YOLO network is tested for robustness.

4. METHODOLOGY

4.1. YOLO Implementations

Four implementations of YOLOv3 were trained using the Darknet Framework [29]. The networks were trained on road training data collected on various road conditions. These implementations include YOLOv3 and Tiny YOLOv3. Two versions of each exist, one for RGB data, and one for IR data. 400 RGB images, and 400 IR images were used for training. These images came from the first two laps of the data collection run. The default YOLO parameters were mostly retained, with the exception of those associated with the number of classes[30].The trained weights were then incorporated into Robotic Operating System (ROS) nodes to handle time syncing with truth data. Additionally, the aspect ratio of the bounding box was considered to reject objects that exceed a threshold as seen below in *Equation 1*.

$$0.8 < \frac{W_y}{H_y} < 1.2 \tag{1}$$

Figure 3: Example of Bounding Box Provided by YOLO

In order to evaluate the robustness of the YOLO implementations, a dataset of approximately 15,000 images of vehicles and roadways was procured. Only the RGB implementations were able to be tested, due to the lack of a dataset of IR images of vehicles. None of the images in the dataset contained the truck which the YOLO implementations were trained on. The goal of the testing was to determine the likelihood of trained networks detecting false positives on images of vehicles that are not the trained vehicle. It should be noted that the dataset consists of images of vehicles in various poses, and might not represent a true driving scenario, which would consist of mainly rear views of vehicles. The results of this analysis can be found in the results section of this paper.

4.2. Pinhole Model

A modified pinhole model was considered as one of the methods for range determination *Equation 2*. Range is defined as *r*, with F_c being the focal length of the camera. *y* is the actual height of the truck in meters, and *y'* is the height of the truck in the image plane. *l* has the units of pixels/meters and is a pixel conversion parameter that handles the conversion of pixels to meters. Similarly c_y is a parameter that handles the translation between the image plane, and the real world. These two parameters must be estimated in order to provide an accurate measurement of range. An erroneous estimate of *l* or c_y disproportionately effects the measurement when the two platooning vehicles at larger ranges, and has less of an effect on closer ranges, this is because of the nonlinear nature of the pinhole camera model.

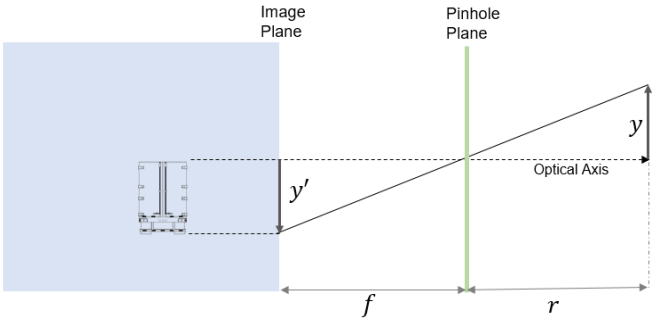

Figure 4: Pinhole Camera Model Graphically Represented

$$r = F_c l \frac{y}{y'} + c_y \tag{2}$$

4.3. Virtual Horizon Model

Park et al.[27] proposed a method for determining monocular range to a vehicle. The proposed method involved computing a virtual horizon, and computing the difference between the bottom of a vehicle and the virtual horizon. According to the source, the method is capable of providing robust range estimation, even when the road inclination varies continuously [27]. The method can be seen represented in the figure below.

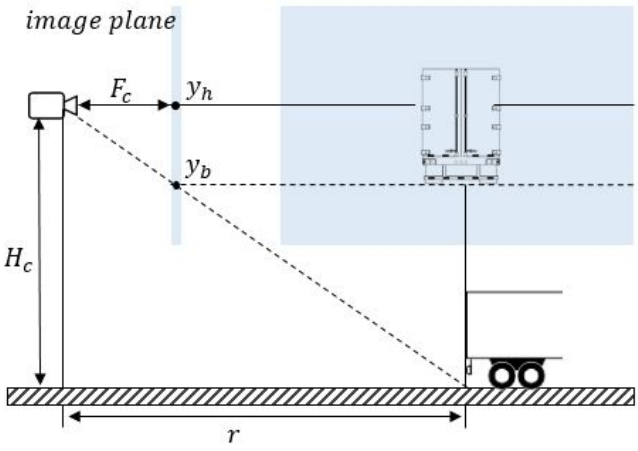

Figure 5: Virtual Horizon Model from [27]

Mathematically, this is represented as:

$$r = \frac{F_c H_c}{y_b - y_h} \tag{3}$$

Where F_c is the focal length of the camera, H_c is the height of the camera, y_b is the y-coordinate of the bottom of the bounding box, and y_h is the virtual horizon line's y-coordinate. y_h is estimated by:

$$y_h = y_b - H_c \frac{w_a}{W_a} \tag{4}$$

Here, w_a is the width of the vehicle in the image plane, and W_a is the actual width of the vehicle in units of length. It should be noted that this work has been improved upon to estimate parameters such as the camera height through the use of lane line detection [28]. This method is not explored here because the width of the lead vehicle is known in this situation, and also it is desired to measure range on roads with and without lane lines. For both ranging methods, range measurements were filtered using a moving average filter which considered the previous 3 measurements.

4.4. Bearing Determination

Using the range to the lead vehicle it is possible to determine the bearing the lead vehicle. First the lateral error between the heading of the follower vehicle, and the lead vehicle is caluclated. This can be done utilizing the range measurement as well as the pinhole camera model. L_e is the lateral error expressed in real world units, L'_e is the lateral error in the image plane which is in pixels. *r* is the range calculated either through the pinhole model, or through the virtual horizon method. *k* is a parameter to handle the real world units to pixel transformation F_c is the focal length of the camera.

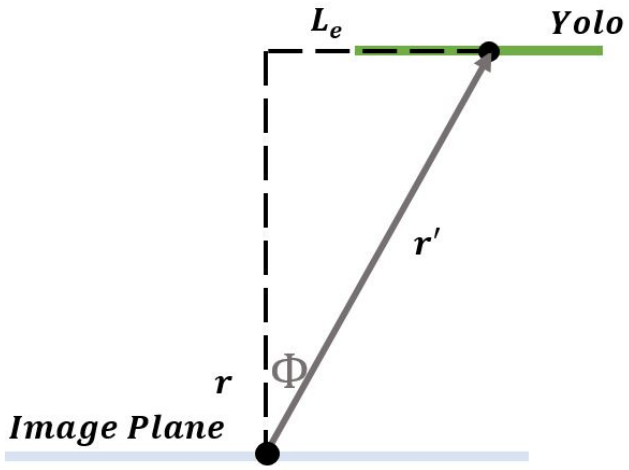

Figure 6: Representation of Bearing Angle

$$L_e = \frac{L'_e r}{F_c k} \tag{5}$$

Once the lateral error has been determined, the angular component of the RPV can be determined by taking the inverse tangent of the lateral error and range.

$$\Phi = arctan(\frac{L_e}{r}) \tag{6}$$

5. DATA COLLECTION

Two Peterbilt 579 commercial trucks were manually driven on road near Auburn University's NCAT facility. These trucks contained GPS receivers (Novatel Propack V3) and radar (Delphi Electronically Scanning Radar - ESR) among other sensors. Camera data was collected through the use of an RGB camera (AXIS P1214-E NET-WORK CAMERA), collected at 1280x720 @ 30 FPS. The IR data was collected using a FLIR Boson Infrared Camera which recorded at 640x480 @ 30 FPS.The ground truth range is provided by the range estimator on Auburn's platform [31], which provides the RPV between the two vehicles. The route traversed can be seen in *figure 7*, along with images depicting the road conditions for each section. Multiple laps

were completed as part of the data collection process. Images from the first two laps were used to train the YOLO models.

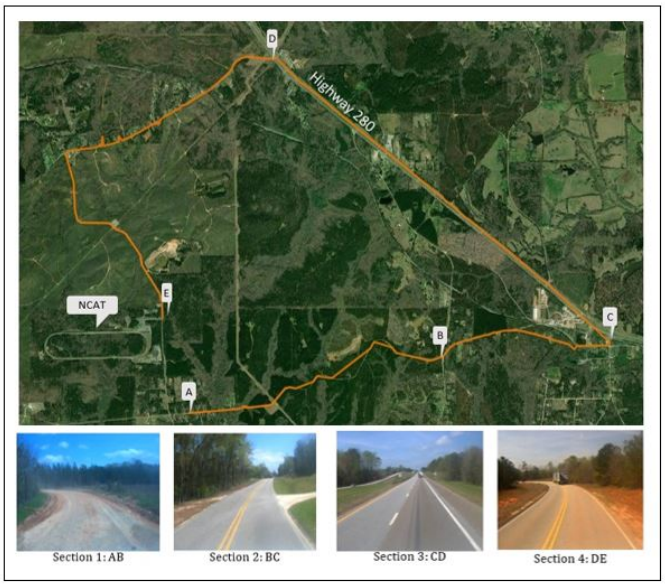

Figure 7: Route taken during testing [Top], and example of various route conditions [Bottom].

6. RESULTS

6.1. YOLO Robustness Evaluation

The YOLO and Tiny YOLO implementations, which were trained on RGB images, were given the vehicle dataset as input to test the false positive rate as outlined in the method section. The vehicle dataset was procured online, which contained over fifteen thousand images of random vehicles in order to gain some understanding of the robustness of the mehtod. The YOLO implementation had a false positive rate of 0.459% and the Tiny YOLO implementation had a false positive rate of 1.21%.

Figure 8: One of the False Positives (70 images out of 15255 for YOLO)

6.2. Range and Bearing Performance

In order to test the algorithms and parameter tuning, image data from the data collection run were used for evaluation. This data came from a modified route which was longer, and was run in the opposite direction in order to evaluate performance on data different than the training data. The range measurements from section 3 of the data collection run can be seen in *figure 9*, along with the DRTK provided measurements which are considered truth. Additionally, the bearing estimates from the same route can be seen in *figure 10*.

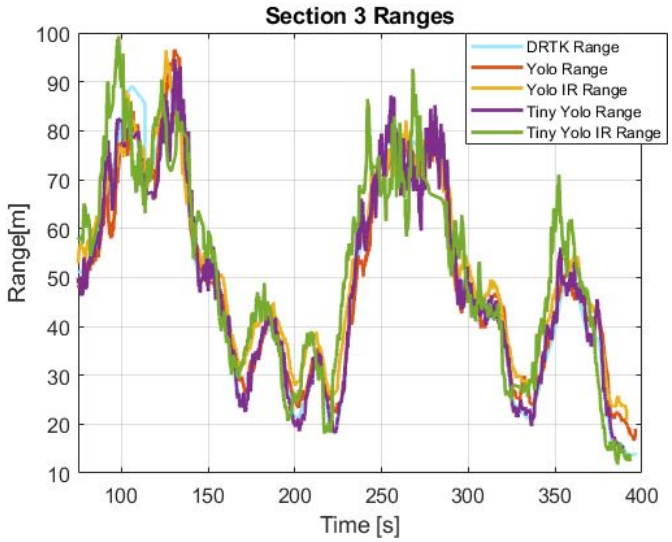

Figure 9: Range Results Using Pinhole Model for Section 3 of on Road Data

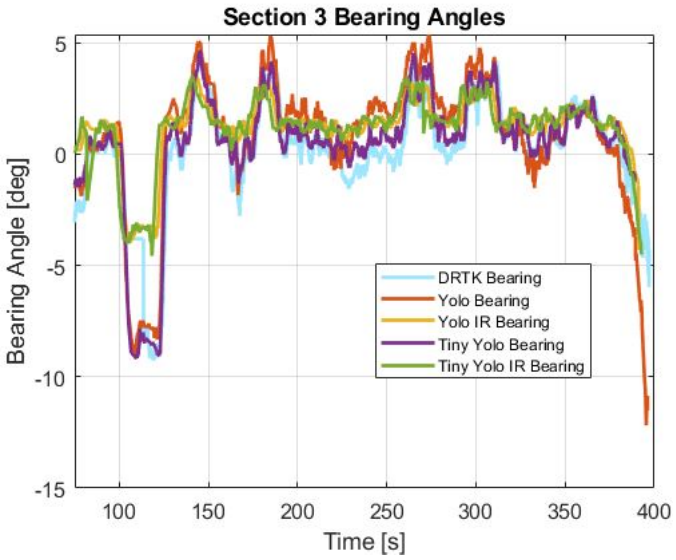

Figure 10: Bearing Results Using Pinhole Model for Section 3 of on Road Data

The two range models applied to Tiny Yolo output data were also compared on a portion of section 1 data. This can be seen in *figure 11*. Additionally, the errors for each model can be seen in *figure 12* for the same portion of the run.

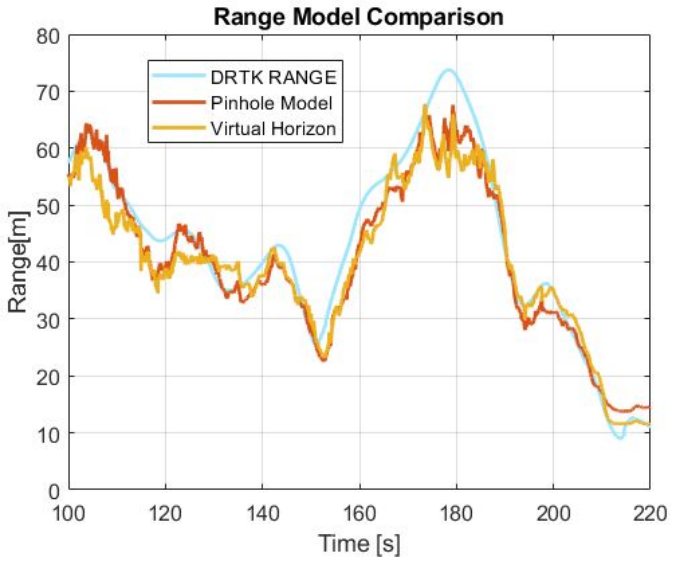

Figure 11: Range from Pinhole Model and Virtual Horizon Method for Section 1 of on Road Data

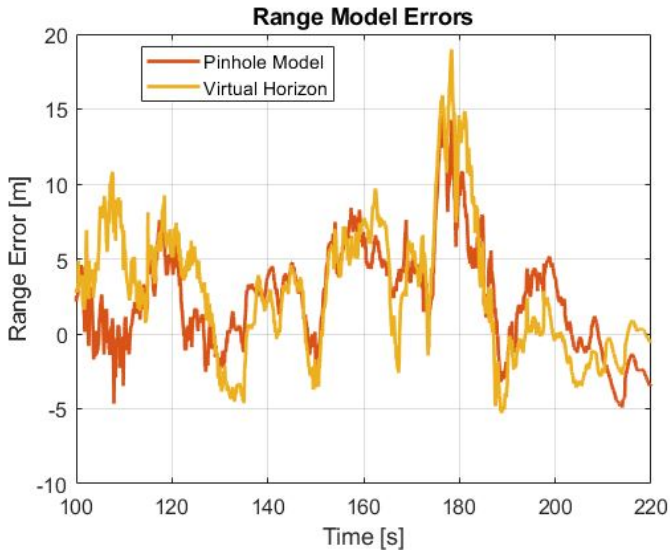

Figure 12: Errors associated with the two range models. It can be seen that the largest errors correspond with large ranges seen in *Figure 11*

To evaluate the performance of the methods, a 2 minute portion of each run was chosen to analyze. The portions were chosen for regions where the DRTK functioned properly, and also where the lead truck remained within 75 meters of the following truck while also remaining in the image frame. An assumption is being made that this would be reasonable to expect for an autonomous platoon which is being controlled around a desired range of less than 75 meters. This dataset was collected using two manually driven trucks, which occasionally exceeded this limit. Additionally, in the event of loss of line of sight, the platoon could continue operation until line of sight to the lead vehicle could be re-established by following lane lines or road edge. The results of this analysis can be seen below in *Table 1*.

Table I: Error for Each Method on Each Section

Mean,Std	Section 1 (Dirt Road)					
	Pinhole Range (m)		Virtual Horizon Range (m)		Bearing Angle (deg)	
Yolo	-2.88	5.08	-2.18	4.83	0.46	1.31
Tiny Yolo	-3.20	3.09	-3.28	3.87	0.48	1.91
Yolo IR	0.53	3.10	0.03	3.14	0.16	3.51
Tiny Yolo IR	-1.66	3.87	-0.41	4.07	0.04	2.26
Mean,Std	Section 2 (Rural Paved)					
	Pinhole Range (m)		Virtual Horizon Range (m)		Bearing Angle (deg)	
Yolo	-3.00	4.09	-0.87	4.12	0.18	0.38
Tiny Yolo	-3.76	3.17	-1.37	2.80	0.20	0.49
Yolo IR	1.82	4.22	-0.10	3.69	-0.17	0.76
Tiny Yolo IR	-1.15	4.22	-0.44	3.50	-0.25	0.96
Mean,Std	Section 3 (Highway 280)					
	Pinhole Range (m)		Virtual Horizon Range (m)		Bearing Angle (deg)	
Yolo	-3.23	3.87	-2.22	3.98	0.34	0.65
Tiny Yolo	-3.88	3.70	-1.93	4.00	0.36	0.77
Yolo IR	1.52	4.36	0.37	3.88	-0.11	1.78
Tiny Yolo IR	0.33	4.29	0.44	3.69	-0.26	1.01
Mean,Std	Section 4 (Rural Paved)					
	Pinhole Range (m)		Virtual Horizon Range (m)		Bearing Angle (deg)	
Yolo	-1.62	2.27	-0.12	2.35	0.52	1.22
Tiny Yolo	-1.50	3.05	-0.90	3.15	0.27	2.09
Yolo IR	1.94	1.99	1.51	1.71	-0.08	1.78
Tiny Yolo IR	3.31	1.65	2.17	2.36	0.21	1.45

Table 1: Errors for each network on each section. Each ordered pair represents the mean and standard deviation respectively

7. DISCUSSION

It can be seen that the methods utilized in this paper closely track the truth range and bearing from DRTK. The average mean and standard deviation for each of the methods can be seen in *Table 2*. The performance difference, with regards to accuracy, between YOLO and Tiny YOLO seems to be marginal when considering all of the runs were with the same camera. However, Tiny YOLO provides measurments at a much faster rate. The range models also seem to perform similarly, with the exception of the virtual horizon model having less mean error while having comparable standard deviation to the pinhole model. The IR camera improvement over RGB for the dirt road can be described as marginally better. Depending on the application, a user would need to decide if this improvement would be worth the additional cost associated with the IR camera.

From *figure11* and *figure 12* it can be seen that the range error appears to correspond to the magnitude of the range. This is likely because both the pinhole model and virtual horizon model are nonlinear equations which can be approximated as linear for a limited range window. Another cause could be that the lead truck becomes indistinguishable from other elements of the image as range increases. This is especially true for IR data which has less features than RGB, including color. This can be seen in *figure 13*, where the lead truck is clearly defined in the first image, and disappears into the background in the second.

Figure 13: Two images from the data collection run. Note that in the second image, the truck is barely visible at long ranges.

Table II: Performance Summary

Mean,Std	All Sections			
	Pinhole Range (m)		Virtual Horizon Range (m)	
Yolo	-2.68	3.83	-1.35	3.82
Tiny Yolo	-3.09	3.25	-1.87	3.46
Yolo IR	1.45	3.42	0.45	3.11
Tiny Yolo IR	0.21	3.51	0.44	3.40
Mean,Std	Bearing Angle (deg)		Other Metrics	
			FPS	RP
Yolo	0.37	0.89	7	0.459
Tiny Yolo	0.33	1.31	30	1.21
Yolo IR	-0.05	1.96	7	--
Tiny Yolo IR	-0.06	1.42	18	--

Table 2: Summary of Results. Each ordered pair represents the mean and standard deviation respectively. FPS is the rate at which the algorithm was capable of running, and RP represents the Robustness Percentage from the robustness testing.

8. CONCLUSION

The work presented here proves the feasibility of monocular vision based platooning on a real world system. The tests were performed on a variety of road conditions, and compares IR and RGB data. Additionally, differing ranging algorithms were explored. The work could be further improved by integrating with other sensors to generate an all encompassing solution that could perform without the need for a GPS solution. These sensors could include Lidar, Radar, or Ultra Wideband Radios (UWBs). Other computer vision algorithms could also benefit the solution, i.e. a lane following solution for a lateral control with an occasional range update from the methods in this paper. Further investigation also needs to be done to evaluate the performance of the algorithms in night-time conditions.

References

[1] S. E. Shladover, "AHS research at the California PATH program and future AHS research needs," in *2008 IEEE International Conference on Vehicular Electronics and Safety*, Sep. 2008, pp. 4–5. DOI: 10.1109/ICVES.2008.4640915.

[2] S. Tsugawa, "Results and issues of an automated truck platoon within the energy ITS project," in *2014 IEEE Intelligent Vehicles Symposium Proceedings*, ISSN: 1931-0587, Jun. 2014, pp. 642–647. DOI: 10.1109/IVS.2014.6856400.

[3] R. Bishop, D. Bevly, J. Switkes, and L. Park, "Results of initial test and evaluation of a Driver-Assistive Truck Platooning prototype," in *2014 IEEE Intelligent Vehicles Symposium Proceedings*, ISSN: 1931-0587, Jun. 2014, pp. 208–213. DOI: 10.1109/IVS.2014.6856585.

[4] S. Tsugawa, S. Jeschke, and S. E. Shladover, "A Review of Truck Platooning Projects for Energy Savings," *IEEE Transactions on Intelligent Vehicles*, vol. 1, no. 1, pp. 68–77, Mar. 2016, Conference Name: IEEE Transactions on Intelligent Vehicles, ISSN: 2379-8904. DOI: 10.1109/TIV.2016.2577499.

[5] S. Martin, "Closely Coupled GPS/INS Relative Positioning For Automated Vehicle Convoys," en, Accepted: 2011-04-15T14:18:41Z, thesis, Apr. 2011. [Online]. Available: https://etd.auburn.edu//handle/10415/2533 (visited on 02/23/2022).

[6] C. Mekik and O. Can, "An investigation on multipath errors in real time kinematic GPS method," *Scientific Research and Essays*, vol. 5, no. 16, pp. 2186–2200, Aug. 2010, Publisher: Academic Journals, ISSN: 1992-2248. DOI: 10.5897/SRE.9000175. [Online]. Available: https://academicjournals.org/journal/SRE/article-abstract/9A7E08A17533 (visited on 02/23/2022).

[7] A. Saxena, "Depth Estimation Using Monocular and Stereo Cues," en, p. 7,

[8] J. Redmon, S. Divvala, R. Girshick, and A. Farhadi, "You Only Look Once: Unified, Real-Time Object Detection," 2016, pp. 779–788. [Online]. Available: https://www.cv-foundation.org/openaccess/content_cvpr_2016/html/Redmon_You_Only_Look_CVPR_2016_paper.html (visited on 02/23/2022).

[9] R. Girshick, J. Donahue, T. Darrell, and J. Malik, "Rich Feature Hierarchies for Accurate Object Detection and Semantic Segmentation," 2014, pp. 580–587. [Online]. Available: https://openaccess.thecvf.com/content_cvpr_2014/html/Girshick_Rich_Feature_Hierarchies_2014_CVPR_paper.html (visited on 04/15/2022).

[10] J. Redmon and A. Farhadi, "YOLOv3: An Incremental Improvement," *arXiv:1804.02767 [cs]*, Apr. 2018, arXiv: 1804.02767. [Online]. Available: http://arxiv.org/abs/1804.02767 (visited on 02/23/2022).

[11] J. Rezgui, É. Gagné, G. Blain, O. St-Pierre, and M. Harvey, "Platooning of Autonomous Vehicles with Artificial Intelligence V2I Communications and Navigation Algorithm," in *2020 Global Information Infrastructure and Networking Symposium (GIIS)*, ISSN: 2150-329X, Oct. 2020, pp. 1–6. DOI: 10.1109/GIIS50753.2020.9248490.

[12] *Kumar,Shankar."Platooning Demonstrator." https://github.com/expectopatronm/platooning-demon (2020).*

[13] Y. Baba, Y. Watanabe, M. Nitta, and K. Kato, "Development of an Adaptive Cruise Control system using a monocular camera," in *2011 11th International Conference on Control, Automation and Systems*, ISSN: 2093-7121, Oct. 2011, pp. 1293–1297.

[14] F. Theinert, T. Coveña, J. Lamers, and D. van Oppenraaij, "Object Tracking for 'Car Platooning' Using a Single Area-Scan Camera," in *2018 19th International Conference on Research and Education in Mechatronics (REM)*, Jun. 2018, pp. 130–135. DOI: 10.1109/REM.2018.8421799.

[15] S. Mitchell, I. Sajjad, A. Al-Hashimi, S. Dadras, R. M. Gerdes, and R. Sharma, "Visual distance estimation for pure pursuit based platooning with a monocular camera," in *2017 American Control Conference (ACC)*, ISSN: 2378-5861, May 2017, pp. 2327–2332. DOI: 10.23919/ACC.2017.7963300.

[16] S. van der Marel, "Development of a Platform for Stereo Visual Odometry based Platooning," en, 2021. [Online]. Available: https://repository.tudelft.nl/islandora/object/uuid%3A1b520436-feed-4a81-8684-ea3d5b1e55e0 (visited on 02/23/2022).

[17] T.-W. Kim, W.-S. Jang, J. Jang, and J.-C. Kim, "Camera and Radar-based Perception System for Truck Platooning," in *2020 20th International Conference on Control, Automation and Systems (ICCAS)*, ISSN: 2642-3901, Oct. 2020, pp. 950–955. DOI: 10.23919/ICCAS50221.2020.9268196.

[18] J. Dichgans, J. Kallwies, and H.-J. Wuensche, "Robust Vehicle Tracking with Monocular Vision using Convolutional Neuronal Networks," in *2020 IEEE International Conference on Multisensor Fusion and Integration for Intelligent Systems (MFI)*, Sep. 2020, pp. 297–302. DOI: 10.1109/MFI49285.2020.9235213.

[19] W. Woeber, "Evaluation of daylight and thermal infra-red based detection for platooning vehicles," *Annals of DAAAM for 2012 & Proceedings of the 23rd International DAAAM Symposium, DAAAM International, Vienna, Austria. 2012.*, 2012.

[20] C. Fries and H.-J. Wuensche, "Autonomous convoy driving by night: The vehicle tracking system," in *2015 IEEE International Conference on Technologies for Practical Robot Applications (TePRA)*, ISSN: 2325-0534, May 2015, pp. 1–6. DOI: 10.1109/TePRA.2015.7219675.

[21] C. Fries, T. Luettel, and H.-J. Wuensche, "Combining model- and template-based vehicle tracking for autonomous convoy driving," in *2013 IEEE Intelligent Vehicles Symposium (IV)*, ISSN: 1931-0587, Jun. 2013, pp. 1022–1027. DOI: 10.1109/IVS.2013.6629600.

[22] C. Fries and H.-J. Wuensche, "Monocular template-based vehicle tracking for autonomous convoy driving," in *2014 IEEE/RSJ International Conference on Intelligent Robots and Systems*, ISSN: 2153-0866, Sep. 2014, pp. 2727–2732. DOI: 10.1109/IROS.2014.6942935.

[23] M. Manz, T. Luettel, F. von Hundelshausen, and H.-J. Wuensche, "Monocular model-based 3D vehicle tracking for autonomous vehicles in unstructured environment," in *2011 IEEE International Conference on Robotics and Automation*, ISSN: 1050-4729, May 2011, pp. 2465–2471. DOI: 10.1109/ICRA.2011.5979581.

[24] *Haseeb, Muhammad Abdul, et al. "DisNet: A novel method for distance estimation from monocular camera." 10th Planning,*

Perception and Navigation for Intelligent Vehicles (PPNIV18), IROS (2018).

[25] S. Khwandah, "Traffic Signs Recognition and Distance Estimation using a Monocular Camera," English, *The 6th International Conference Actual Problems of System and Software Engineering: IEEE*, pp. 407–418, Dec. 2019, Publisher: CEUR Workshop Proceedings (CEUR-WS.org). [Online]. Available: https://pure.solent.ac.uk/en/publications/traffic-signs-recognition-and-distance-estimation-using-a-monocul (visited on 02/23/2022).

[26] G. Stein, O. Mano, and A. Shashua, "Vision-based ACC with a single camera: Bounds on range and range rate accuracy," in *IEEE IV2003 Intelligent Vehicles Symposium. Proceedings (Cat. No.03TH8683)*, Jun. 2003, pp. 120–125. DOI: 10.1109/IVS.2003.1212895.

[27] K.-Y. Park and S.-Y. Hwang, "Robust Range Estimation with a Monocular Camera for Vision-Based Forward Collision Warning System," en, *The Scientific World Journal*, vol. 2014, e923632, Jan. 2014, Publisher: Hindawi, ISSN: 2356-6140. DOI: 10.1155/2014/923632. [Online]. Available: https://www.hindawi.com/journals/tswj/2014/923632/ (visited on 04/13/2022).

[28] A. Ali, A. Hassan, A. R. Ali, H. U. Khan, W. Kazmi, and A. Zaheer, "Real-time vehicle distance estimation using single view geometry," 2020, pp. 1111–1120. [Online]. Available: https://openaccess.thecvf.com/content_WACV_2020/html/Ali_Real-time_vehicle_distance_estimation_using_single_view_geometry_WACV_2020_paper.html (visited on 04/13/2022).

[29] J. Redmon, *Darknet: Open Source Neural Networks in C*, 2013. [Online]. Available: https://pjreddie.com/darknet/ (visited on 04/13/2022).

[30] *Mahendran, Vino. "Custom object training and detection with YOLOv3, Darknet and OpenCV." https://blog.francium.tech/custom-object-training-and-detection-with-yolov3-darknet-an 41542f2ff44e. (2019).*

[31] J. Ward, P. Smith, D. Pierce, *et al.*, "Cooperative Adaptive Cruise Control (CACC) in Controlled and Real-World Environments: Testing and Results," English, American Center for Mobility, Tech. Rep., Aug. 2019. [Online]. Available: https://www.osti.gov/biblio/1834377 (visited on 04/15/2022).